

2017A ALUMINUM ALLOY IN DIFFERENT HEAT TREATMENT CONDITIONS

K. Mroczka^{1)*}, A. Wójcicka¹⁾, P. Kurtyka¹⁾

¹⁾ *Department of Technology and Engineering of Material, Institute of Technology, Pedagogical University of Cracow, Poland*

Received 07.05.2012

Accepted 13.07.2012

* *Corresponding author: e-mail: kmroczka@up.krakow.pl, Tel./fax (04812) 638-25-21, Institute of Technology, Pedagogical University of Cracow, Poland, ul. Podchorążych 2, 30-084 Kraków*

Abstract

Aluminium alloy 2017A is a precipitation-hardened material. The paper includes the results of studies on the effect of different heat treatment conditions on the alloy. The most proper temperature for solution treatment of the alloy is 500 °C (the acceptable temperature range is between 490 °C and 520 °C). The maximum hardness and the highest ultimate tensile strength as a result of natural aging was obtained after 72 hours. Artificial aging at 180 °C causes a sufficient increase in hardness after 6 hours. Natural aging of the material causes increases the ultimate tensile strength by 20% (compared to the supersaturation state).

Keywords: aluminum alloys, precipitation, tensile test, hardness, fracture

1 Introduction

The use of aluminum alloys in the modern world is already widespread and it can be assumed that it will increase. This is due to the demand for lightweight high-strength, mainly in construction and transport industries [1, 2]. Technically pure aluminum has good formability, good thermal conductivity but very little strength. Increasing the strength of aluminum can be achieved in several ways: by solid-solution-hardening, precipitation-hardening [3] or by refinement of grains (according to Hall-Petch relationship [4]), creating a fine and even ultrafine grains microstructure (eg. grain size less than 0,5 µm). However, precipitation-hardening is the most effective method. This type of hardening is often used in aluminum alloys containing copper, magnesium, chromium, lithium, zinc [5, 6]. The efficiency of particle interaction with dislocations is dependent on several factors, including: dispersity, the number and size of precipitates, the type and location of precipitates in the microstructure. Precipitations coherent with the matrix which are located inside the grains are the most effective. Due to the different methods of production of aluminum components (casting, extrusion, rolling [7, 8]) or processing (welding [3, 9]), the creation of an optimum microstructure in a single technology process is extremely difficult and additional heat treatment is necessary. For most commercial alloys, i.e. the ones commonly produced in a diverse assortment, and also composites with aluminum matrix [10, 11], the developed recommendations to the heat treatment give the best strengthening results. The most commonly given information applies only to the temperature range of supersaturation and aging, but it does not give time specifications of the aging process. It is very important to note that too long artificial aging can lead to so-called overaging i.e. decreased strength and hardness of the material as a result of, mostly, coagulation of the precipitates. The knowledge of the recommended treatment temperature as well as the time of

this process are essential for optimum hardening results. With regard to the ranges of the heat treatment temperature, deviations from specified ranges and the impact of the implementation of treatment at a slightly higher or slightly lower temperature should be known. This is important due to the industrial and even the laboratory practice because one has to take into account *e.g.*: thermal inertia of the furnace - temperature drop after the introduction into the furnace of a material of greater weight and overheated above the set point temperature, when the control of the furnace is trying to rapidly increase the temperature to a specified value.

The aim of the study whose results are presented below was to determine the effect of different supersaturation temperatures and aging on the strengthening of aluminum alloy 2017A.

2 Material and experimental methods

The studied material is aluminum alloy EN AW-2017A (PN-EN: 573-3:2009). This aluminum alloy is used for plastic working. The main alloying addition is copper and therefore the alloy is classified within the group of 2XXX series alloys. The chemical composition of the material presented in table 1 while table 2 shows the mechanical properties respectively.

Designation of aluminum alloy EN AW-2017A according to other standards (counterparts) [12]:

- Designation with respect to chemical symbols according to BS EN: 573-3: AlCu4MgSi(A)
- Designation according to PN-79/H-82160:PA6
- Designation according to DIN: AlCuMg1
- Werkstoff No.: 3.1325

Table 1 The chemical composition of the material - alloy EN AW-2017A

Cu	Mg	Mn	Si	Fe	Zn	Cr
3.9	0.6	0.6	0.4	0.7	0.25	0.1

Table 2 The mechanical properties of alloy EN AW-2017A - for a specific state of treatment

State	R _{p0.2} [MPa]	R _m [MPa]	A5 [%]	Hardness [HV]
0	70	180	13 – 20	50
T4	230 - 275	380 - 425	10 – 21	115
T6	250	400	10	130

State:

0 – annealed – for products obtained with specified properties after hot-production

T4 – heat treated – supersaturated and naturally aged to a stable state

T6 – heat treated – supersaturated and then artificially aged.

In order to determine the effect of heat treatment parameters of the material on the mechanical properties the following experiments and tests were performed:

- supersaturation samples from different temperatures between 470 and 530 °C, then cooled in water,
- natural aging of supersaturated samples at temperatures from 470 to 530 °C
- artificial aging of samples at temperatures of 140, 160, 180 °C which were supersaturated of 500 °C /water,
- strength testing (static tensile test),
- hardness testing,

- studies of the microstructure of fractures of selected samples broken in the static tensile test,
- studies of the microstructure (light microscopy) of selected samples.

The sheet of 6 mm thick of aluminum alloy 2017A-T6, industrially produced was used in the studies. Samples with dimensions of 20 x 20 mm were cut out.

Heat treatment (supersaturation and artificial aging) was performed by heating the samples in a laboratory chamber furnace with digital control. Hardness measurement was carried out using Vickers method, with the load of 10 kG (10 kG = 98.07 N). Prior to the hardness measurement, the samples were subjected to grinding, in order to remove oxide layers formed during the heat treatment.

Static tensile test were performed on a testing machine INSTRON TT-DM 10T with digital control. Testing samples with dimensions of $l_0 = 20$ mm, $l = 57$ mm, $d = \phi 4$ mm were cut out from the sheet in the direction parallel to the direction of rolling, according to the standard round samples. The samples were mounted axially in the chuck and were stretched with traverse speed of $V_t = 0,01$ mm/s. Under the adopted parameters of the sample, strain rate was:

$$\bullet \quad \varepsilon = \frac{1}{l_0} \cdot V_t = \frac{1}{20} \cdot 0.01 = 0.0005 \left[\frac{1}{s} \right] \quad (1.)$$

Tensile tests were conducted at ambient temperature.

A microscopic examination was performed on fracture by scanning using the electron microscope SEM Philips M525. All the samples underwent fracture in the static tensile test. The microstructure examination was performed using the Olympus GX51 light microscope equipped with Nomarski contrast and software for archiving and imaging analysis. The preparation of the samples for observation consisted of metallographic specimens on the surface (of the sheet) and the cross-section. The samples were grinded and polished mechanically. Disclosure of the microstructure was obtained in two ways: by etching in HF+HNO₃+H₂O and by etching in an aqueous solution of NaOH (a concentration of which was chosen experimentally by etching the samples sequentially with solutions, whose concentration was increased by adding to the existing solution a few grams of NaOH).

3 Results and discussion

The results of hardness measurements of the samples after supersaturation at temperature of 470, 480, 490, 500, 510, 520 and 530 °C are presented in Fig. 1 in the form of a black line. Analysis of these results shows relatively small differences in hardness of the individual samples from 89 ÷ 109 HV10. The highest hardness was obtained for the sample supersaturated at 480 °C (109 HV10). The samples treated with the temperature in the range from 490 °C to 510 °C have reduced hardness of about 98 HV10, which explains the temperature scope cited in the literature (the range of supersaturation temperature 500 ÷ 510 °C [12,13]).

Graphs in **Fig. 1** also show the results of the hardness measurements of these samples (after supersaturation at the temperature ranging from 470 °C to 530 °C) made after 24, 48, 72 hours, the average of the measurements after 96 and 120 hours and after 62 days of the supersaturation (the aging temperature of about 20 °C). After 24 hours from the time of supersaturation of the samples an increase in hardness from 17 HV10 to 36 HV10 (on average of 26 HV10) is observed. Subsequent measurements made after 48 and 72 hours show a lower rate of increase in

hardness in relation to the first 24 hours. The resulting hardness is comparable, but the greatest was obtained after 72 hours. Data analysis showed that supersaturation of the material at 500 °C causes an increase in hardness to a maximum value of 144 HV10. However, it can be noted that supersaturation in the temperature range between 490 °C and 520 °C results in similar hardness of the material as the one obtained after aging for over 48 hours. It is therefore a greater temperature range than the one recommended in the literature (500 – 510 °C [12]). The influence of a long-term natural aging process (62 days) on hardness of supersaturated samples is presented in **Fig. 2**. One can note that the results for samples supersaturated at the temperature of 490 °C and higher are similar (about 130 HV10).

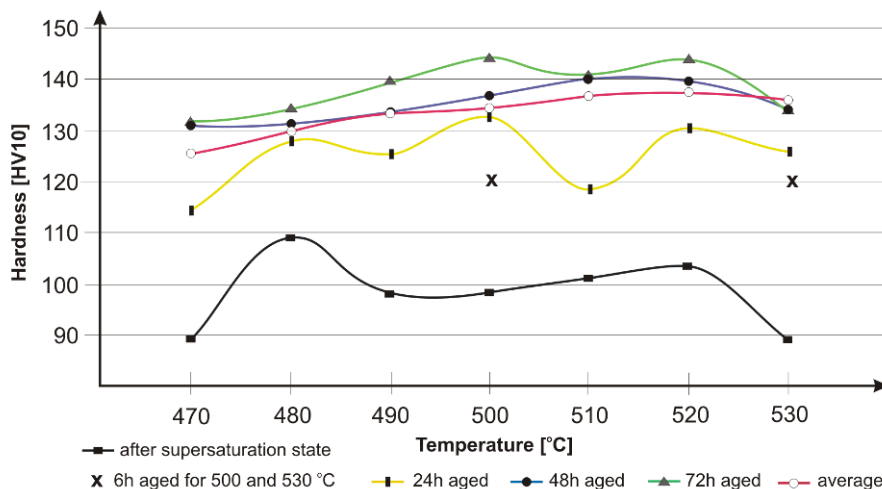


Fig. 1 The results of hardness measurements made at different times of the natural aging of the supersaturated samples from the temperature range between 470 and 530 °C (average – average of measurement results at 96, 120 hours and 62 days)

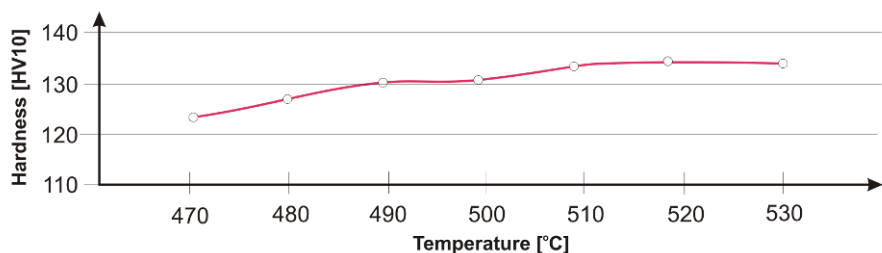


Fig. 2 The results of hardness measurements made after 62 days of natural aging of supersaturated samples from the temperatures range between 470 and 530 °C

As a complement to the above analysis, the results of the measurements are presented in a form graph in **Fig. 3**. The highest hardness was designated in red; keep in mind that the chart is based on data for each temperature and time. One can only assume that the values between the data points vary roughly in proportion.

Additionally, next samples supersaturated at 500 and 530 °C were examined after less than 24 hours – the results Fig. 1 (mark x). Results of the supersaturated sample at 500 °C showed that the increase in hardness on about 20 HV10 was observed already after six hours of the natural aging process. The remaining results are similar to those previously obtained. An analysis of the results for the supersaturated sample at temperature of 530 °C shows the same hardness (120HV10) after 6 hours of natural aging but a larger increase in hardness as hardness of the material after supersaturation was about 10 HV lower (89.2 HV10). For other times of aging (like for sample 500 °C), the results are similar to previously described studies.

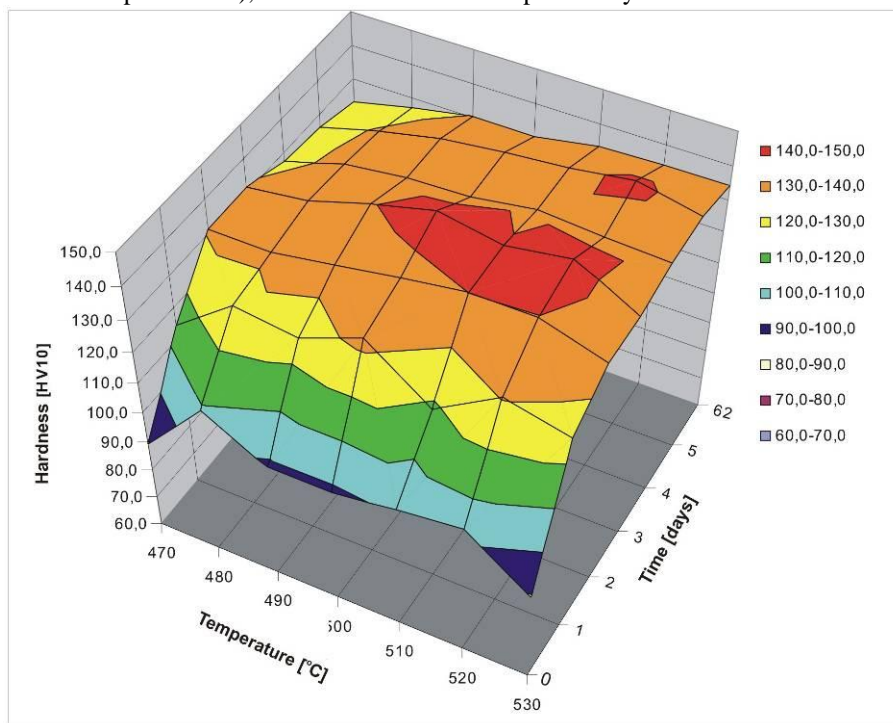


Fig. 3 Summary results of hardness measurements made at different times of the natural aging supersaturated samples at the temperatures between 470 °C and 530 °C

Artificial aging was performed at temperatures of 140, 160 and 180 °C on samples supersaturated from 500 °C (water cooling). Hardness tests were performed on samples sequentially removed from the furnace after the aging time of: 1, 2, 4, 6, 8, 10, 13, 16, 20, 26, 32, 40, 48, 56, 64 hours. The measurement results are shown in Fig. 4.

In the case of all the three aging temperatures, the increase in hardness of the material has been observed, while for the samples ageing at temperature 140°C and 160°C the increase in hardness is slower and heterogeneous – after about 8 hours a decrease in hardness of the samples followed by the re-growth has been observed (**Fig. 4**). The fastest increase in the hardness is observed for the sample aged at the temperature of 180 °C, which can be explained by the most intense diffusion due to high temperature. The highest hardness, which however was reached after a relatively long time (52 hours), is obtained in the sample aged at the temperature of 160 °C. Further studies show that in the case of the eight-hour aging process (technologically aging time which is frequently used), the process temperature should be 180 °C because by applying this

temperature and after the specified time the achieved hardness is comparable to the hardness achieved during a treatment process lasting longer. It can be also stated that for this temperature of the aging the sufficient time to obtain the correct hardness is 6 hours.

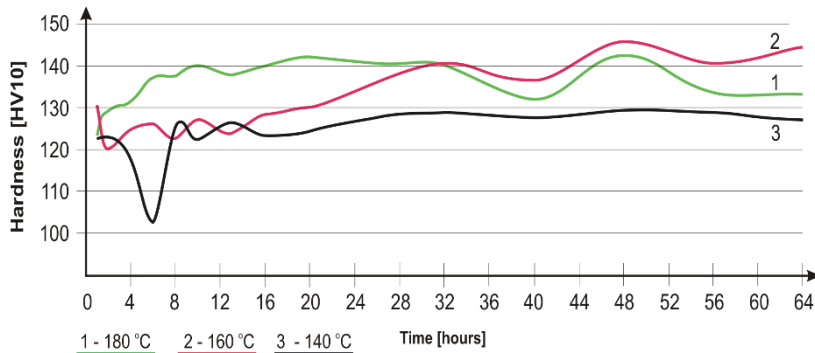


Fig. 4 The results of hardness measurements of samples artificially aged

Fig. 5 shows collective results for tensile samples in the initial states, after supersaturation, after natural aging and after artificial aging. The analysis of the curves demonstrates a similar way of flow of the material and the strengthening of all samples except the artificially aged ones. The curve for this sample shows much less plasticity. As expected, the greatest plasticity and the lowest proof stress and tensile strength were shown by the sample in the state after supersaturation. The material in this state should be mostly a supersaturated solution without any significant amount of strengthening precipitates, but it is solution-strengthened. An excess of

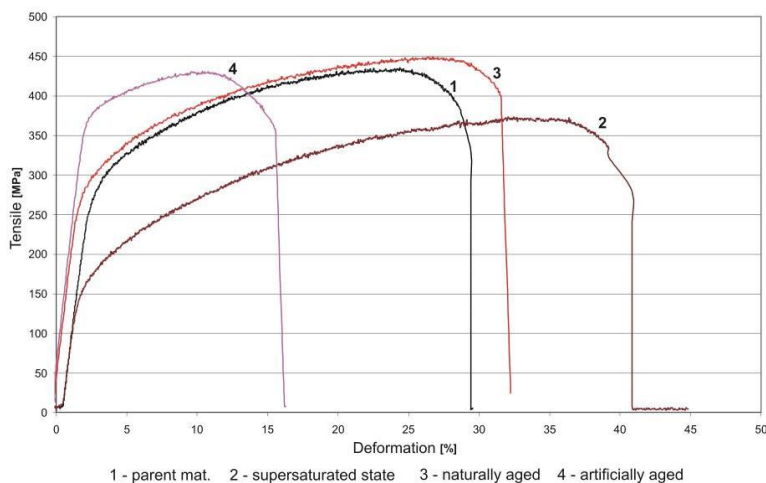


Fig. 5 Graphs stress-strain dependence (obtained in static tensile test), for the material in state: baseline, after supersaturation, after natural aging and after artificial aging

copper, which is present in the solution of aluminum will increase stresses in the crystal lattice aluminum, which impede the movement of dislocations during plastic deformation. This kind of consolidation is much less effective than strengthening precipitation with secreting phase from a

supersaturated solution. The effects of such precipitation hardening (finely dispersed phase spontaneously forming from a supersaturated solution) are shown for a sample in naturally aged specimens, whose strength ($R_{p0.2} = 270$ MPa, $R_m = 449$ MPa) is much greater than in case of the sample in the supersaturated state (Fig. 5, Table 3). Comparison of curves of the samples at initial and after natural aging showed a very similar shape, although the sample after natural aging has greater strength and greater ductility. This is in line with the expectations because the initial material is in the T6 condition, *i.e.* after artificial aging. However, we failed to obtain from the manufacturer of sheet metal information on the exact parameters of heat treatment of the material during the process of its production. The results of strength tests are summarized in **Table 3**. The results obtained for the endurance (strength) tests correlate with the results of hardness testing of samples in each state.

Table 3 The obtained results of strength tests of samples in different state

Samples state	$R_{0.2}$ [MPa]	R_m [MPa]	R_u [MPa]	A [%]	Z [%]
initial	250	436	622	22	39
after supersaturation	150	374	596	28	44
after natural aging	270	449	680	24	41
after artificial aging	361	431	609	13	41

R_u – actual stress in the breaking sample

The analysis was performed using a scanning electron microscope (SEM). **Fig. 6** shows examples of areas of the sample in the state after supersaturation. The tensile curve for this sample shows the plasticity of this material but to a limited extent. This is confirmed by observations of the fractures, where one can see the effects of plastic deformation mainly in microareas (Fig. 6a).

Relative comparison of the analyzed surface with the results of samples observation in the initial state indicates participation of smaller number of particles in the process of cracking (which can be observed in fracture) which is in line with expectations, since the sample is in the supersaturated state. Evaluation of chemical composition of particles on the basis of the characteristic X-ray spectrum of the EDS detector indicates brittle particles of $-Al_xMn_yFe_z$ type (for example: Al_2FeMn_3 or $Al_6(MnFe)$) and dissolved copper (Fig. 6a). In addition, the presence of particles rich in aluminum and copper (probably phase Al_2Cu) is noted (Fig. 6b). This indicates that the supersaturation process did not cause complete dissolution of the larger particles containing copper. This condition may result from an insufficiently long time of annealing of the sample above the solvus temperature (about 60 minutes). One must remember that the dissolution rate of particles is associated with the diffusion rate of released atoms from the particles, in this case copper, in the matrix, *i.e.* in the aluminum lattice. The fact that diffusion occurs not in pure aluminum, but only in the Al-Cu solution also contributes to the slowing down of the process. Copper comes from nanometric strengthening precipitates earlier dissolved in the matrix. Additionally, a few particles involving aluminum and magnesium were also observed at the fractures. Moreover, the effects of plastic deformation in the form of so-called craters (Fig. 6a – top of the photo) or surfaces on which slip bands are visible, are noted around several particles (Fig. 6a – marked by the arrow). It can be assumed that these areas are likely grain boundaries, which were deformed during tension with the disclosed slip bands on their surfaces. In general, the observed fracture can be described as ductile but not as much as is observed in materials with high plasticity, such as Cu [14].

Observations of breakthroughs in the states of the initial and after aging lead to similar conclusions as above, except that a larger number of segregations in the breakthroughs was observed.

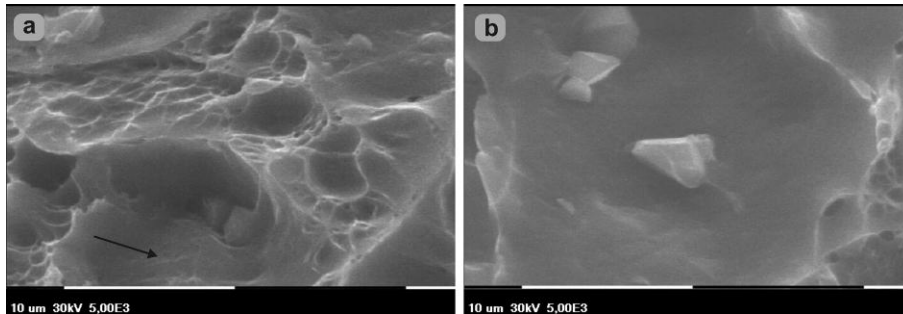


Fig. 6 SEM micrograph of the fracture of the tensile tested sample after supersaturation: a) typical ductile fracture with brittle precipitation contain Al, Fe, Mn surrounded by slip bands marked by the arrow, b) precipitation contain Al, Cu

Microstructure of the alloy (light microscopy), in the so-called delivery status (T6) of material *i.e.* without any additional heat treatment (supersaturation, aging) were analyzed. In Fig. 7, the surface microstructure disclosed by etching with NaOH-based solution is shown. An analysis of the microstructure shows the presence of precipitates of different size (above 1 µm). These are the segregations of different types, which can be determined on the basis of color that has been obtained by etching and the light beam of light microscope. Differentiation of the phases is even more apparent when the observation is made in the interference-differential contrast by Nomarski (**Fig. 7**). However, identification of the phase is not possible using this research technique, though it appears that there will be mainly $Al_xFe_yMn_z$ -type precipitates which are commonly found in aluminum alloys and larger precipitates of the phase occurring in the series 2XXX alloys (Al_2Cu [15] or S' Al_2CuMg [16], previously mentioned in the description of research fractures. Smaller precipitates are also located at grain boundaries.

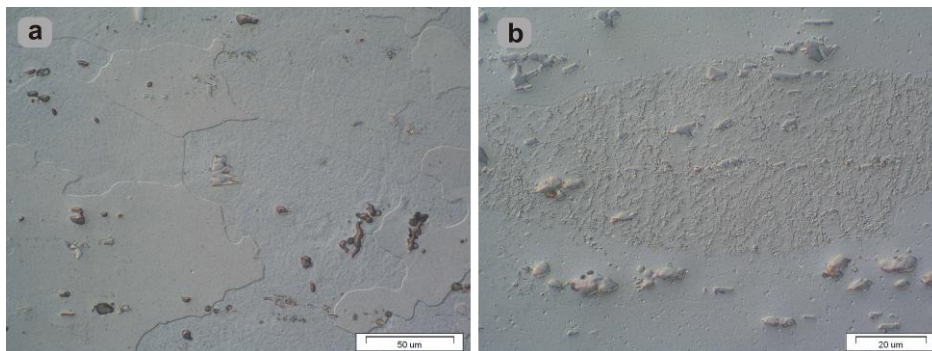


Fig. 7 The microstructure (light microscopy - Nomarski contrast) of the parent material (initial state) etched NaOH: a) on the plate surface, b) on the cross-section

The analysis of the microstructure on the cross-section confirms the above observation and indicates strips layout of the segregations inside the materials which is typical for rolled items. Moreover, in Fig. 7b (observation in differential – interference contrast) one of the areas clearly

distinguishable against the background of the material matrix. This appearance of the microstructure is likely the result of the characteristic crystallographic orientation occurring in this area as compared to other grains due to the different intensity of etch reagent impact.

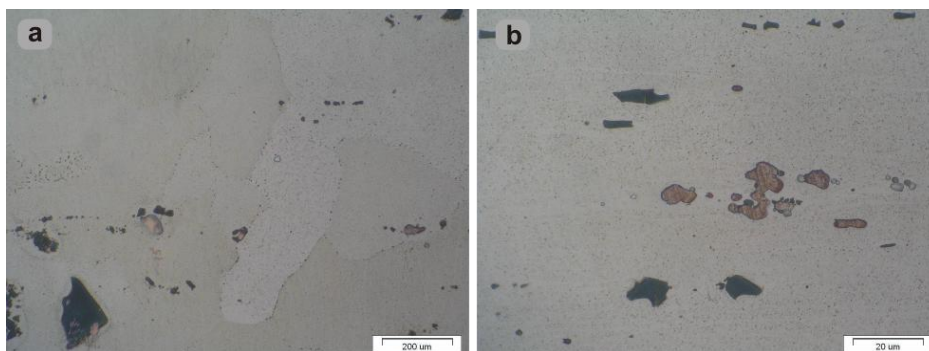


Fig. 8 The microstructure (light microscopy) of the parent material (initial state) etched HF+HNO₃: a) on the plate surface, b) on the cross-section

In **Fig. 8**, the microstructure of the above described samples analyzed on the surface and cross-section, however etched with solution based on HF and HNO₃, is shown. Observations confirm the previously-given descriptions, i.e. the ones about the occurrence of different phases in the material, however the phase visible earlier as fair now changed its color to dark due to the process of digestion. This method of etching allowed to the explicit disclosure of the precipitates located at grain boundaries (Fig. 8a). Moreover, banding of the microstructure is visible better, which concerns not only the larger precipitates (Fig. 8b).

4 Conclusions

On the basis of experiments and studies the following conclusions are formulated:

- The temperature range for the process of supersaturation is 490 ÷ 520 °C, the optimum temperature: 500 °C;
- The highest hardness of the material (144 HV10) after the natural aging process has been obtained for quenched sample after solution annealing at 500 °C, which has been aged for 72 hours;
- The greatest increase in hardness (up to 146 HV10) as a result of the artificial aging process occurs when the temperature is 160 °C, but only after 48-hour annealing;
- The fastest growth in hardness (max. hardness (142 HV10) after 20 hours the of annealing) occurred in the material aged at temperature of 180 °C;
- For the typical time of treatment of artificial aging (8 hours), the greatest increment in hardness was obtained in the material aged at temperature of 180 °C (137 HV10);
- The highest tensile strength (449 MPa) and the greatest breaking stress of material (680 MPa) was obtained for the material naturally aged; proof stress of the material is 270 MPa;
- The material artificially aged at the optimal parameters (180 °C / 8 hours) shows similar tensile strength as the material in the initial state (431 MPa), but much higher proof stress (361 MPa);
- The smallest tensile strength (374 MPa), proof stress (150 MPa) and the greatest plasticity (28%) of the material are obtained in the state after supersaturation.

References

- [1] A. Francesconi, D. Pavarin, C. Giacomuzzo, F. Angrilli: International Journal of Impact Engineering, Vol. 33, 2006, No. 1-12, p. 264-272
- [2] J. J. M. de Rijck, J. J. Homan, J. Schijve, R. Benedictus: International Journal of Fatigue, Vol. 29, 2007, No. 12, p. 2208-2218
- [3] Y. S. Sato, S. H. C. Park, H. Kokawa: Metallurgical and Materials Transactions A, Vol. 32a, 2001, No. 12, p. 3033-3042
- [4] Y. D. Huang, Y. L. Liu, P. Wambua: Journal of Materials Science, Vol. 36, 2001, No. 19, 4711-4717
- [5] M. K. Banerjee: Journal of Materials Science, Vol. 32, 1997, No. 24, p. 6645-6651
- [6] B. C. Wei, C. Q. Chen, Z. Huang, Y. G. Hang: Materials Science and Engineering A, Vol. 280, 2000, No.1, p. 161-167
- [7] M. S. Kaiser, S. Datta, A. Roychowdhury, M. K. Banerjee: Materials Characterization, Vol. 59, 2008, No. 11, p. 1661-1666
- [8] J. S. Robinson, T. Y. Liu, A. K. Khan, M. J. Pomeroy: Journal of Materials Processing Technology, Vol. 209, 2009, No. 6, p. 3069-3078
- [9] K. Mroczka, A. Pietras: Archives of Material Science and Engineering, vol. 40, 2009, No. 2, p. 104-109
- [10] P. Kurtyka, Y-C. Yoo, S. Wierzbiński: Proc. of IVth Int. Conf. Non- Ferrus Metals and Alloys, Cracow, Poland, 1999
- [11] P. Kurtyka, M. Faryna, S. Wierzbiński: Composites, 2002, No. 4, p. 185-190
- [12] L. A. Dobrzański et al.: *Dictionary of material science. Metals, polymers, ceramics and composites*. Verlag Dashofer, Warsaw, 2006 (in Polish)
- [13] G. P. Dolan, J. S. Robinson: Journal of Materials Processing Technology, Vol. 153-154, 2004, p. 346-351
- [14] A. Kováčová, T. Kvačkaj, M. Kvačkaj, T. Donič, M. Martikán, M. Besterici: Acta Metallurgica Slovaca, Vol. 15, 2009, No. 2, p. 100-104
- [15] B. Kužnicka: Materials Characterization, Vol. 60, 2009, No. 9, p. 1008-1013
- [16] E. Dryzek, J. Dryzek: Tribology International, Vol. 39, 2006, No. 7, p. 669-677